Numerical Analysis of Rarefied Gas Flow Induced around a Flat Plate with a Single Heated Side

Satoshi Taguchi* and Kazuo Aoki†

*Organization of Advanced Science and Technology, Kobe University, Kobe 657-8501, Japan
†Department of Mechanical Engineering and Science, and Advanced Research Institute of Fluid Science and Engineering, Graduate School of Engineering, Kyoto University, Kyoto 606-8501, Japan

Abstract. A rarefied gas flow induced around a flat plate with a uniformly heated single side in a closed vessel, which is also known as the radiometric flow, is considered. Its steady behavior is investigated on the basis of the Bhatnagar-Gross-Krook (BGK) model of the Boltzmann equation and the diffuse reflection boundary condition for a wide range of the Knudsen number, by means of an accurate finite-difference method which gives a correct description of the discontinuity contained in the velocity distribution function. It is found that a thermal edge flow is induced along the plate on both heated and unheated sides near the edge, that drives the overall circulating flow in the vessel. The detailed flow structure near the edge as well as along the plate is clarified.

Keywords: Rarefied gas flow, thermal edge flow, radiometric force
PACS: 47.45.-n, 51.10.+y, 05.20.Dd, 47.56.+r

INTRODUCTION

Let us consider a flat vane immersed in a rarefied gas rested in a closed vessel. If the temperatures of two sides of the vane are different, a force is exerted on it, resulting in a motion of the vane with the hotter side trailing. This phenomenon is known as the radiometric phenomenon and can be observed in the famous Crookes radiometer. This classical phenomenon [1, 2, 3] has received significant attention in modern kinetic theory [4] in relation to various applications in microtechnologies (see the references in [4]). It is known that the source of the force is the rarefied gas flow caused by the temperature field around the vane.

On the other hand, when a uniformly heated plate is immersed in a rarefied gas, a flow called the thermal edge flow is induced near the edges [5, 6]. Since the vanes in radiometers are thin, this flow may play an important role in the flow structure in radiometers. However, this aspect has not been paid attention to so far. In the present study, focusing on this aspect, we carry out an accurate numerical analysis of the flow around an infinitely thin plate in a radiometer by a finite difference method based on a model Boltzmann equation.

PROBLEM AND FORMULATION

We consider a rarefied gas confined in a square vessel $-L/2 \le X_1 \le L/2$ and $-L/2 \le X_2 \le L/2$ with a uniform temperature T_0, where X_i is the rectangular space coordinate system (Fig. 1). An infinitely long flat plate with width D and without thickness is placed in the gas at $X_1 = 0$ and $-D/2 \le X_2 \le D/2$. The surface of the plate facing the negative X_1 direction ($X_1 = 0_-$ and $-D/2 \le X_2 \le D/2$) is kept at the same temperature as the vessel, whereas that facing the positive X_1 direction ($X_1 = 0_+$ and $-D/2 \le X_2 \le D/2$) is kept at a different uniform temperature T_1 higher than T_0 ($T_1 > T_0$). We investigate the steady behavior of the gas induced in the vessel under the following assumptions: (i) the behavior of the gas is described by the Bhatnagar-Gross-Krook (BGK) model of the Boltzmann equation; (ii) the gas molecules reflected on the boundaries obey the diffuse reflection condition.

Basic Equations

Let us first introduce the following notations: ξ_i (or $\boldsymbol{\xi}$) denotes the molecular velocity, $f(X_1, X_2, \boldsymbol{\xi})$ the velocity distribution function, $\rho(X_1, X_2)$ the density, $v_i(X_1, X_2)$ the flow velocity ($v_3 = 0$), $T(X_1, X_2)$ the temperature, and R the specific gas constant (the Boltzmann constant divided by the mass of a molecule). Then, the BGK equation for the

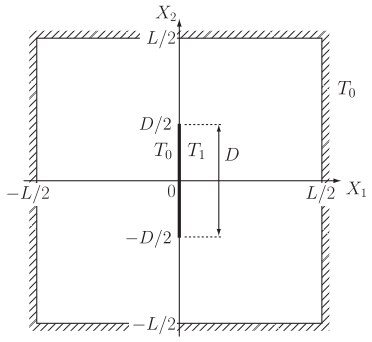

FIGURE 1. Problem.

present steady two-dimensional problem is written as

$$\xi_1 \frac{\partial f}{\partial X_1} + \xi_2 \frac{\partial f}{\partial X_2} = A_c \rho (f_e - f), \quad f_e = \frac{\rho}{(2\pi RT)^{3/2}} \exp(-\frac{(\xi_j - v_j)^2}{2RT}), \tag{1}$$

$$\rho = \int f d\boldsymbol{\xi}, \quad v_i = \frac{1}{\rho} \int \xi_i f d\boldsymbol{\xi}, \quad T = \frac{1}{3R\rho} \int (\xi_j - v_j)^2 f d\boldsymbol{\xi}, \tag{2}$$

where A_c is a constant ($A_c\rho$ is the collision frequency), $d\boldsymbol{\xi} = d\xi_1 d\xi_2 d\xi_3$, and the integral with respect to $\boldsymbol{\xi}$ is carried out over the whole space. Let us denote by S^+ and S^- the right- and left-hand sides of the plate, respectively. That is, $S^\pm = \{(X_1, X_2) \mid X_1 = 0_\pm,\ -D/2 \le X_2 \le D/2\}$. The diffuse reflection condition on each side of the plate is given by

$$f = \frac{\sigma_w^\pm}{(2\pi RT_w^\pm)^{3/2}} \exp(-\frac{\xi_j^2}{2RT_w^\pm}) \quad \text{for } \pm\xi_1 > 0 \quad (\text{on } S^\pm), \tag{3}$$

$$\sigma_w^\pm = \mp(\frac{2\pi}{RT_w^\pm})^{1/2} \int_{\pm\xi_1<0} \xi_1 f(X_1 = 0_\pm, X_2, \boldsymbol{\xi}) d\boldsymbol{\xi}, \tag{4}$$

where $T_w^+ = T_1$ and $T_w^- = T_0$ and the upper (lower) sign corresponds to S^+ (S^-). On the other hand, the boundary condition on the container [$(X_1 = \pm L/2,\ -L/2 \le X_2 \le L/2)$ or $(-L/2 < X_1 < L/2,\ X_2 = \pm L/2)$] is given by

$$f = \frac{\sigma_w}{(2\pi RT_0)^{3/2}} \exp(-\frac{\xi_j^2}{2RT_0}) \quad \text{for } \xi_j n_j > 0, \quad \text{with} \quad \sigma_w = -(\frac{2\pi}{RT_0})^{1/2} \int_{\xi_j n_j<0} \xi_j n_j f d\boldsymbol{\xi}, \tag{5}$$

where n_i ($n_3 = 0$) is the unit normal vector to the boundary pointing to the gas.

Let us introduce other macroscopic variables, the pressure p and the stress tensor p_{ij}. They are defined by

$$p = R\rho T, \quad p_{ij} = \int (\xi_i - v_i)(\xi_j - v_j) f d\boldsymbol{\xi}. \tag{6}$$

The present boundary-value problem is characterized by the parameters L/D, T_1/T_0, and the Knudsen number $\mathrm{Kn} = \ell_0/D$, where $\ell_0 = (2/\sqrt{\pi})(2RT_0)^{1/2}/A_c\rho_{av}$ is the mean free path of the gas molecules in the equilibrium state at rest with temperature T_0 and density ρ_{av} with ρ_{av} being the average density of the gas in the vessel. In RESULTS AND DISCUSSIONS below, the notation $p_0 = R\rho_{av}T_0$ is also used.

NUMERICAL ANALYSIS

Since the problem is symmetric with respect to $X_2 = 0$, we can analyze it in the upper half domain ($X_2 \ge 0$) by imposing the specular reflection boundary condition at $X_2 = 0$, i.e.,

$$f(X_1, 0, \xi_1, \xi_2, \xi_3) = f(X_1, 0, \xi_1, -\xi_2, \xi_3) \quad \text{for } \xi_2 > 0 \quad (-L/2 < X_1 < L/2). \tag{7}$$

Then, the solution in the lower half domain $X_2 < 0$ is given in terms of that in the upper half domain by $f(X_1, X_2, \xi_1, \xi_2, \xi_3) = f(X_1, -X_2, \xi_1, -\xi_2, \xi_3)$ $(-L/2 \le X_1 \le L/2,\ -L/2 \le X_2 < 0)$.

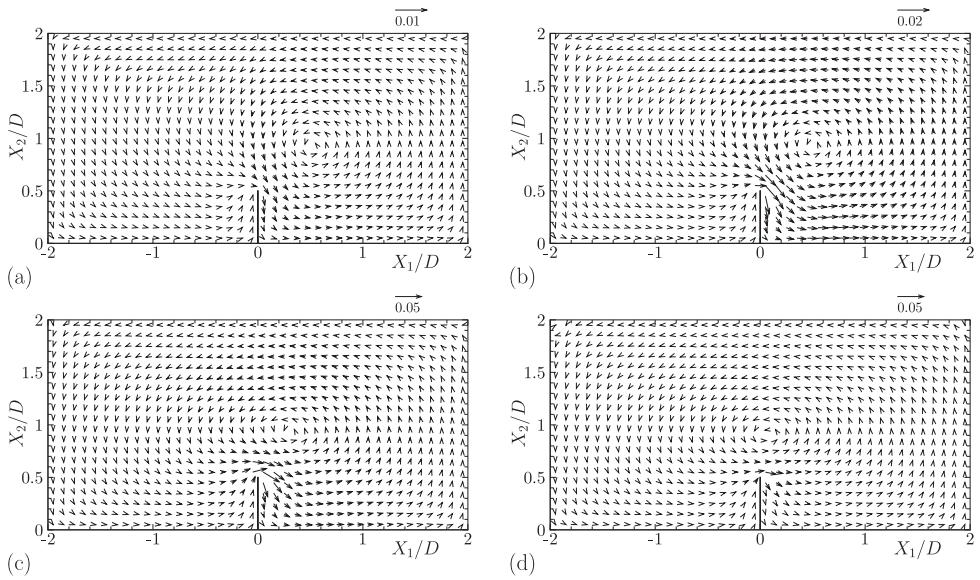

FIGURE 2. The flow induced in the upper half of the vessel for $T_1/T_0 = 2$. (a) Kn $= 5$, (b) Kn $= 1$, (c) Kn $= 0.1$, (d) Kn $= 0.01$. The arrow indicates the two-dimensional flow velocity vector $(v_1, v_2)/(2RT_0)^{1/2}$ at its starting point.

We analyze the present boundary-value problem by the finite difference method introduced in [7], where a supersonic rarefied gas flow past a flat plate has been investigated. It is well known that the velocity distribution function is generally discontinuous in the gas around a convex boundary [8]. The same holds true in the present problem, where the convex nature is concentrated at the edges of the plate. That is, for any fixed ξ_i, a discontinuity is introduced in the velocity distribution function at each edge and it propagates in the gas along the characteristic of (1). Consequently, at any point (X_1, X_2) in the gas, the velocity distribution function is discontinuous in the direction $\xi_2/\xi_1 = (X_2/D \mp 1/2)/(X_1/D)$ on any plane $\xi_3 = const$ in the $\boldsymbol{\xi}$ space [the upper (lower) sign corresponds to the discontinuity originating from $(X_1/D, X_2/D) = (0, 1/2)$ and $(0, -1/2)$, respectively]. The situation is the same in the case of the flow past a flat plate, and the method of [7] is capable to capture such discontinuities. It should also be mentioned that the discontinuity is also caused by the four corners of the vessel. However, since this discontinuity is much smaller than that caused by the edge, we ignore it in our numerical analysis. Since the detailed description of the numerical method is given in [7], we omit it here and concentrate on the results.

RESULTS AND DISCUSSIONS

The computation is carried out for $L/D = 4$ and $T_1/T_0 = 2$, and for the Knudsen number Kn ranging from 0.01 to 20. Figures 2–4 show, respectively, the flow velocity, isodensity lines, and isothermal lines in the upper half of the vessel for various Kn. A counterclockwise circulating flow is induced. At the location away from the edge, the flow speed increases as Kn decreases, and then decreases. The center of the circulation shifts toward $X_1 = 0$ with the decrease of Kn. The isolines of the macroscopic variables meet at the edge. This is because the macroscopic variables are not determined uniquely there. That is, they take different values at the edge depending on the direction of approach. The flow speed takes its maximum in the close vicinity of the edge in all the cases. Near the edge appear steep temperature gradients along the plate on both heated and unheated sides, each of which causes a flow along the plate by the same mechanism as the thermal creep flow. Such flows are known as the thermal edge flow [5, 6]. The flow is in the downward (upward) direction on the right-hand side (left-hand side) of the plate. In the free molecular limit Kn $= \infty$, no flow is induced in the vessel, as proved in [9].

In order to see more closely the flow field near the edge as well as along the plate, we show in Figs. 5 and 6 the profiles of some macroscopic quantities along the X_2 axis for various Kn (Fig. 5 for Kn $= 5$, 1, and 0.5; Fig. 6 for Kn $= 0.1$, 0.05, and 0.01). In each figure, (a) shows the profile of the flow speed $|v_i| = (v_1^2 + v_2^2)^{1/2}$, (b) that of the temperature T, and (c) that of the pressure p. Note that $v_1 = 0$ on the plate $(0 \le X_2/D \le 1/2)$ and that $|v_i| = |v_2|$ there. Note also that the macroscopic quantities are discontinuous at the edge (see the previous paragraph). In the

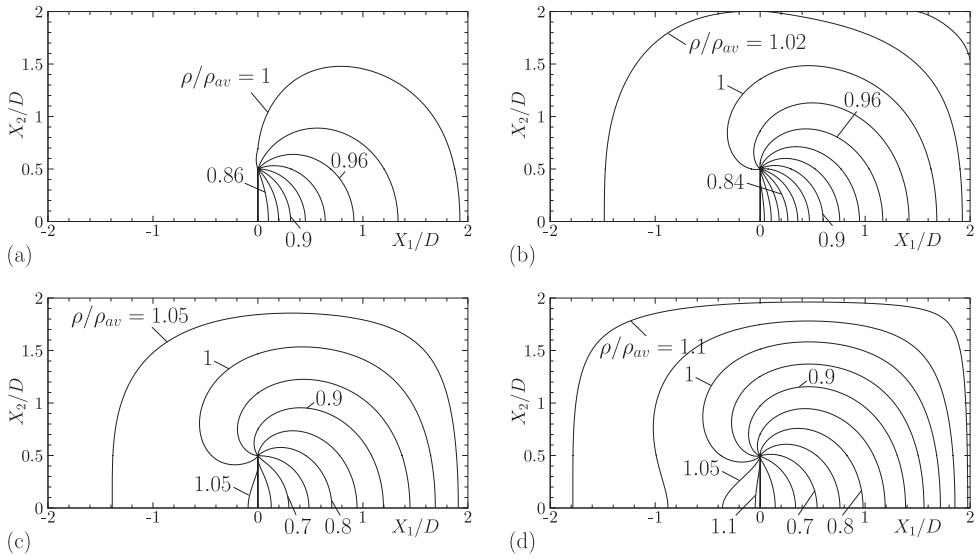

FIGURE 3. Isodensity lines in the upper half of the vessel for $T_1/T_0 = 2$. (a) Kn $= 5$; $\rho/\rho_{av} = 0.86 + 0.02m$ ($m = 0, \ldots, 7$), (b) Kn $= 1$; $\rho/\rho_{av} = 0.78 + 0.02m$ ($m = 0, \ldots, 13$), (c) Kn $= 0.1$; $\rho/\rho_{av} = 0.65 + 0.05m$ ($m = 0, \ldots, 8$), (d) Kn $= 0.01$; $\rho/\rho_{av} = 0.6 + 0.05m$ ($m = 0, \ldots, 10$).

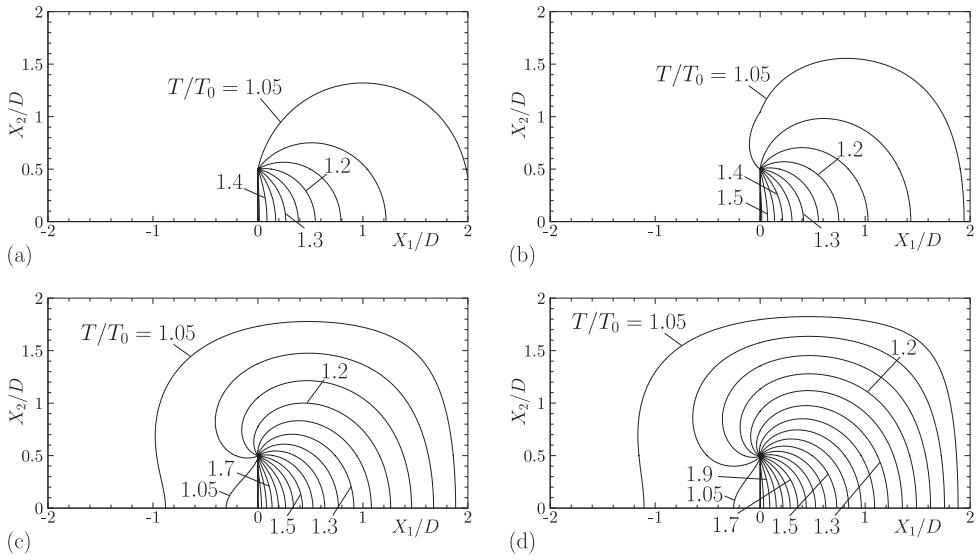

FIGURE 4. Isothermal lines in the upper half of the vessel for $T_1/T_0 = 2$. (a) Kn $= 5$; $T/T_0 = 1.05 + 0.05m$ ($m = 0, \ldots, 8$), (b) Kn $= 1$; $T/T_0 = 1.05 + 0.05m$ ($m = 0, \ldots, 10$), (c) Kn $= 0.1$; $T/T_0 = 1.05 + 0.05m$ ($m = 0, \ldots, 15$), (d) Kn $= 0.01$; $T/T_0 = 1.05 + 0.05m$ ($m = 0, \ldots, 18$).

free molecular flow (Kn $= \infty$), the macroscopic quantities are uniform along each side of the plate. The velocity distribution of the impinging molecules on the plate is isotropic and no tangential force is exerted. The molecular collisions thermalize the molecules impinging on the plate on the heated (right-hand) side, causing a temperature rise there [Fig. 5(b)]. Near the edge, the gas is cooled down (heated up) on the right-hand (left-hand) side of the plate due to the slower (faster) molecules coming from the negative (positive) X_1 direction. Therefore, the temperature is more elevated in the middle part of plate on the right-hand side and near the edge on the left-hand side. In these hotter regions, faster molecules tend to repel each other, causing the decrease of the density (or the gas is expanded there). In this way, a nonuniform pressure distribution along the plate with a high (low) pressure region near the edge on the right-hand (left-hand) side is established [see Fig. 5(c)]. The velocity distribution of the impinging molecules

being disturbed nonuniformly, it is no longer isotropic and a tangential force is exerted on the plate. As its reaction, a flow is induced. The flow speed increases with the decrease of Kn [Fig. 5(a)]. With the further decrease of Kn, the flow velocity tends to vanish and the temperature tends to accommodate to the surface temperature in the bulk part of the plate [Fig. 6(a) and (b)]. However, the state of the gas is far from equilibrium in the vicinity of the edge where the surface temperatures changes discontinuously. Therefore, near the edge, the near-free-molecular type behavior described above is retained locally. This nonequilibrium region seems to be confined in the edge area whose width is of the order of the mean free path, and thus it becomes vanishingly thin in the limit Kn $\to 0$. However, our numerical results indicate that the values of the macroscopic quantities at the edge are not likely to approach the corresponding values in the bulk part of the plate, where the state of the gas approaches a uniform equilibrium state on each side as Kn $\to 0$.

In the first paragraph of the present section, we stated that thermal edge flows with upward and downward directions are induced on heated and unheated sides of the plate, respectively. Then, one may ask if a similar flow pattern is obtained near the edge if one considers the problem of the original thermal edge flow in which both sides of the plate are equally heated (or cooled). In order to verify this, we also performed numerical computations by setting the temperature of S^- (the left-hand side of the plate) equal to T_1 ($T_1 = 2$ or 0.5). Though two problems are quite different and a direct comparison is not possible, it has been found that the local flow structure on the heated side (unheated) side in the present problem is similar to that of the original thermal edge flow around a heated (cooled) plate. Especially, the temperature and pressure (or density) fields exhibit a striking resemblance between two problems. Thus, it is almost certain that the thermal edge flow is induced in the present problem and plays an essential role.

Let us denote by $(F,0,0)$ the total force acting on the plate (per unit width in X_3). Then, F is given by $F = -2\int_0^{D/2}[p_{11}]^+_-dX_2$, where $[p_{11}]^+_- = (p^+_{11} - p^-_{11})$ with $p^\pm_{11} = p_{11}(X_1 = 0_\pm, X_2)$. In Fig. 7, we show the distribution of the normal stress p_{11} along the plate for various Kn [(a)] and F versus Kn [(b)] ($T_1/T_0 = 2$). The distribution of p_{11} is similar to that of the pressure p, including the way of transition with respect to Kn [cf. Figs. 5(c) and 6(c)]. When Kn is large, the force is exerted on the whole part of the plate. As Kn becomes small, the difference of the normal stress $[p_{11}]^+_-$ between both sides vanishes in the bulk part of the plate and the force acts only on the edge area, which tends to shrink with the decrease of Kn. As a result, the total force F vanishes in the limit Kn $\to 0$, in spite of the fact that the stress difference remains finite at the edge in the same limit (see the last sentence of the second paragraph of this section). The total force F increases monotonically with Kn and reaches the limiting value $F/Dp_0 = -0.20986$ in the free molecular limit (Kn $\to \infty$).

Finally, we summarize some data for the present numerical computation. Here, we use the dimensionless variables $x_i = X_i/D$ and $\zeta_i = \xi_i/(2RT_0)^{1/2}$. For the discretization of the (x_1,x_2) space, the upper half domain is subdivided by (321,161) nonuniformly distributed lattice lines [for the (x_1,x_2) directions]. The minimum lattice interval is 2.8×10^{-5} (Kn $= 0.01$), 6.7×10^{-5} ($0.02 \le$ Kn ≤ 0.05), 8.4×10^{-4} ($0.06 \le$ Kn ≤ 1), and 3.7×10^{-3} ($1.5 \le$ Kn ≤ 20) for both the x_i direction ($i = 1,2$). For the $\boldsymbol{\zeta}$ space, we first eliminate the ζ_3 variable from the system by taking marginals of f. Then, (ζ_1,ζ_2) is expressed by the plane polar coordinates as $(\zeta_1,\zeta_2) = (\zeta\cos\theta_\zeta, \zeta\sin\theta_\zeta)$. The discretization is made on (ζ,θ_ζ) and we have used (73×481) grid points (nonuniform for ζ and uniform for θ_ζ). The minimum interval for ζ grid is 2.0×10^{-3} at $\zeta = 0$, and the maximum interval is 0.35 at $\zeta = 8.58$, which is the upper limit of ζ. In order to estimate the accuracy of the present computation, we compared the result based on the standard lattice system with that based on a finer lattice system containing double lattice lines both for the x_1 and x_2 directions. The differences in the macroscopic variables (relative for ρ, T, and p, and absolute for u and v) are less than 2.7×10^{-4} for Kn $= 0.1$ and less than 8.5×10^{-5} for Kn $= 0.5$, 1, 2, 5, 10, and 20 in the whole domain. A similar comparison was also made for the (ζ,θ_ζ) space. Since the variations in the macroscopic variables for this case were much smaller than the corresponding variations in the test for the (x_1,x_2) space, the values are omitted here.

REFERENCES

1. Reynolds, O., *Phil. Trans. R. Soc. Lond.* **166**, 725–735 (1876).
2. Maxwell, J. C., *Phil. Trans. R. Soc. Lond.* **170**, 231–256 (1879).
3. Kennard, E. H., *Kinetic Theory of Gases*, McGraw-Hill, New York, 1938.
4. Selden, N., Ngalande, C., Gimelshein, S., Muntz, E. P., Alexeenko, A., and Ketsdever, A., *Phys. Rev. E* **79**, 041201 (2009).
5. Aoki, K., Sone, Y., and Masukawa, N., "A Rarefied Gas Flow Induced by a Temperature Field," in *Rarefied Gas Dynamics*, edited by Harvey, J., and Lord, G., Oxford Univ. Press, Oxford, 1995, pp. 35–41.
6. Sone, Y., and Yoshimoto, M., *Phys. Fluids* **9**, 3530–3534 (1997).
7. Aoki, K., Kanba, K., and Takata, S., *Phys. Fluids* **9**, 1144–1161 (1997).
8. Sone, Y., and Takata, S., *Transp. Theory Stat. Phys.* **21**, 501–530 (1992).

9. Sone, Y., *J. Méc. Théor. Appl.* **3**, 315–328 (1984); *ibid.* **4**, 1–14 (1985).

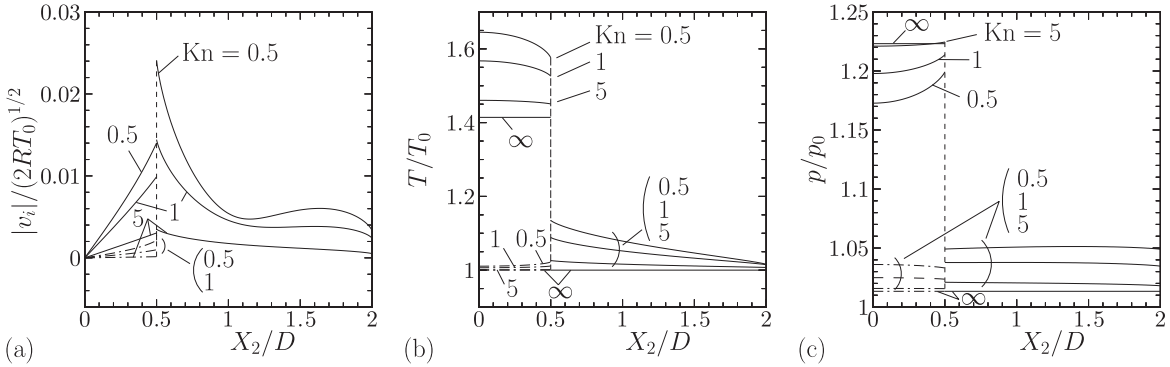

FIGURE 5. Profiles of the flow speed $|v_i| = (v_1^2 + v_2^2)^{1/2}$, temperature T, and pressure p along the X_2 axis for various Kn (Kn = 5, 1, and 0.5) for $T_1/T_0 = 2$ in the case of $L/D = 4$. (a) $|v_i|$, (b) T, (c) p. The result for the positive side of the plate ($X_1 = 0_+$ and $0 \le X_2/D \le 1/2$) is shown by the solid line and that for the negative side ($X_1 = 0_-$ and $0 \le X_2/D \le 1/2$) by the dash-dotted line. In (b) and (c), the result for the free molecular flow (Kn $\to \infty$) is also included.

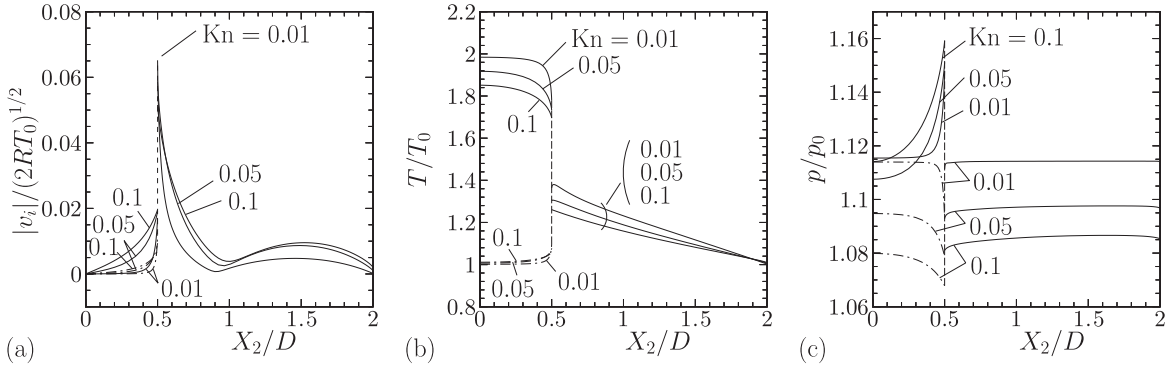

FIGURE 6. Profiles of the flow speed $|v_i| = (v_1^2 + v_2^2)^{1/2}$, temperature T, and pressure p along the X_2 axis for various Kn (Kn = 0.1, 0.05, and 0.01) for $T_1/T_0 = 2$ in the case of $L/D = 4$. (a) $|v_i|$, (b) T, (c) p. The result for the positive side of the plate ($X_1 = 0_+$ and $0 \le X_2/D \le 1/2$) is shown by the solid line and that for the negative side ($X_1 = 0_-$ and $0 \le X_2/D \le 1/2$) by the dash-dotted line.

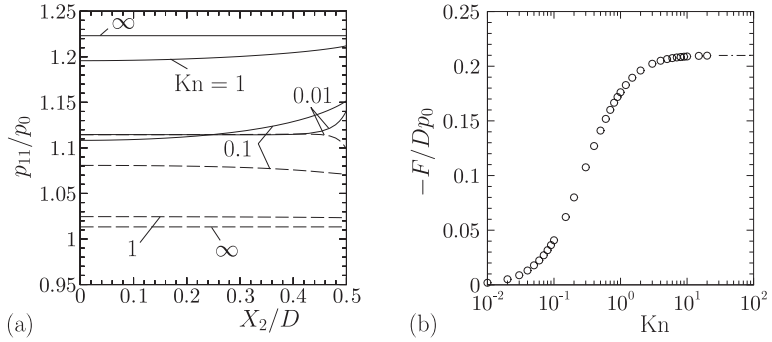

FIGURE 7. Distribution of the normal stress p_{11} along each side of the plate [(a)] and the force F acting on the plate [(b)] for $T_1/T_0 = 2$ in the case of $L/D = 4$. In (a), the result for the positive side of the plate ($X_1 = 0_+$ and $0 \le X_2/D \le 1/2$) is shown by the solid line and that for the negative side ($X_1 = 0_-$ and $0 \le X_2/D \le 1/2$) by the dashed line. The result for the free molecular flow (Kn $\to \infty$), which is constant in X_2, is also shown in (a). In (b), the limiting value $F/Dp_0 = -0.20986$ in the free molecular limit (Kn $\to \infty$) is indicated by the dash-dotted line.